Journal of Crystal Growth 318 (2011) 411–414

Contents lists available at ScienceDirect

Journal of Crystal Growth

journal homepage: www.elsevier.com/locate/jcrysgro

Numerical simulation of ammonothermal growth processes of GaN crystals

Yan-Ni Jiang [a], Qi-Sheng Chen [a,*], V. Prasad [b]

[a] Institute of Mechanics, Chinese Academy of Sciences, 15 Bei Si Huan Xi Road, Beijing 100190, China
[b] University of North Texas, P.O. Box 311277, Denton, TX, USA

ARTICLE INFO

Available online 18 November 2010

Keywords:
A1. Convection
A1. Fluid flow
A1. Growth models
A2. Ammonothermal growth
B1. GaN

ABSTRACT

Gallium nitride (GaN) is a semiconductor material with a wide array of applications in the manufacture of blue/green light LEDs, lasers and high power electronic devices. In the ammonothermal growth, ammonia is used as a solvent instead of water as in the hydrothermal process. We modeled ammonothermal growth of GaN crystal of 1 in. size in a cylindrical high-pressure autoclave and discussed the effects of the different baffle design. We can conclude that, under the condition of forward solubility, the small opening is not in favor of the crystal growth. When the opening increases from 12% to 16%, the flow direction in the central hole changes from positive to negative. In the cases of 16% and 20% openings the flow in the autoclave exhibits a steady circulation, so the growth is stable. The transfer of raw material depends on the baffle opening and the temperature difference between growth zone and dissolving zone.

1. Introduction

High-quality GaN substrate can be used to fabricate next-generation light-emitting diodes (LEDs) and laser diodes (LDs); therefore many researchers investigate nitride crystal growth. There are many methods to grow GaN crystals such as high-pressure solution growth [1], low-pressure solution growth with flux [2] and ammonothermal growth [3]. A promising method is the ammonothermal technique pioneered by Dwilinski et al. [4,5] and further being developed by Ketchum and Kolis [6], Purdy [7] and Yoshikawa et al. [8]. The ammonothermal technique is drawn from the hydrothermal technique widely used to grow quartz. The autoclave of ammonothermal crystal growth system is filled with high-pressure and high-temperature ammonia. A baffle is used to divide the inner autoclave into two zones—an upper zone and a lower zone. The two zones are heated independently, and the heater is controlled to maintain the lower zone at a higher temperature than the upper zone. It is difficult to perform any measurement of the temperature and flow rate, and numerical simulation is an effective tool for studying the ammonothermal crystal growth process.

Chen et al. [9–11] investigated the ammonothermal GaN single-crystal process by numerical simulation extensively. They studied the effects of retrograde solubility and forward solubility on the fluid flow pattern and temperature distribution around the baffle, the effect of particle size on the nutrient transport and the effects of the baffle design. Pendurti et al. [12] investigated the influence of the geometric and the thermal boundary conditions of the system on the growth rate of crystal. Recently, Masuda et al. [13] investigated the effect of funnel-shaped baffle on the heat transfer in 2 in. crystals growth system, but they did not give the influence of different openings. Up to now, however there is no report about the effect of the opening of baffle on the flow rate.

Natural convection is important to ammonothermal crystal growth process. It can transport the dissolved raw material from the lower zone to the upper zone. The baffle, which divides the autoclave into two parts—upper and lower portions, can control the heat and mass transfer rate. So in this paper, we considered an ammonoacidic condition with an internal diameter of 1.75 in. in which GaN has normal solubility and discussed the effects of the different baffle design. The system is modeled using fluid dynamics, thermodynamics and heat transfer models.

2. Physical and mathematical model

In the ammonothermal growth, predetermined amount of ammonia, mineralizers and GaN particles are loaded in the bottom of an autoclave, while seeds are hanged on a ladder made from Pt wire above a baffle with certain opening (Fig. 1). Mineralizers were used to obtain a solubility of GaN in supercritical ammonia. The baffle is made from 0.28 mm thick Pt foil and used to divide the autoclave into two parts—upper and lower portions. The part of the autoclave below the baffle is applied with a high temperature, T_H, and the part of the autoclave above the baffle is applied with a low temperature, T_L: two strap heaters are used on the sidewall of autoclave to obtain the required temperatures. A temperature gradient is achieved on the sidewall of the autoclave, 300–250 °C from the bottom to the top of the sidewall. In this paper, we

* Corresponding author. Tel.: +86 10 82544092.
E-mail address: qschen@imech.ac.cn (Q.-S. Chen).

0022-0248/$ - see front matter © 2010 Elsevier B.V. All rights reserved.
doi:10.1016/j.jcrysgro.2010.10.218

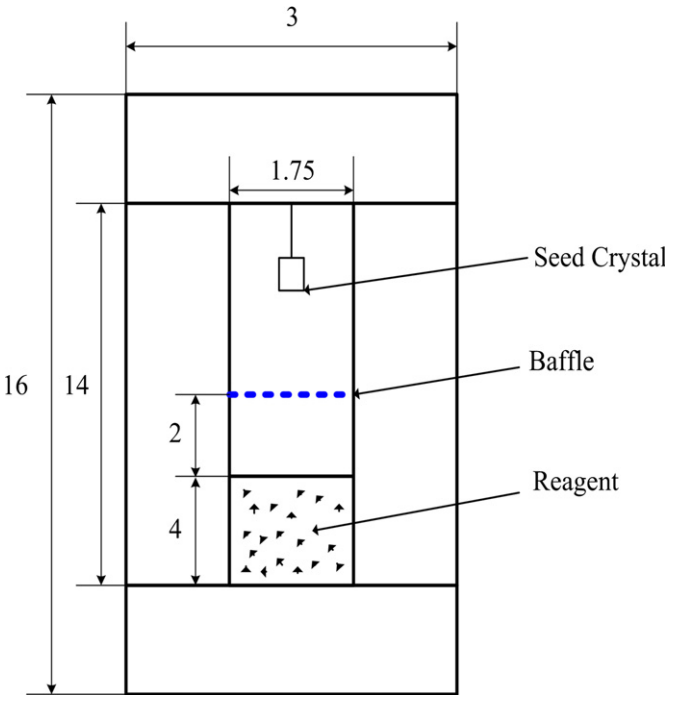

Fig. 1. Schematic of an ammonothermal growth system.

consider a case in which the autoclave has an internal diameter of 1.75 in. (4.44 cm), external diameter of 3.875 in., internal height of 14 in. (35.56 cm) and external height of 18 in. The charge height is 4 in. (10 cm), and the charge particle size is 0.6 mm. The baffle is located at a distance of 6 in. from the bottom of the autoclave. The maximum temperature difference applied on the sidewall of the autoclave is 50 K.

The nutrient particles (GaN) in the bottom of the autoclave can be considered as a porous medium. In this case, the Darcy–Brinkman–Forchheimer model can be employed in the porous layer. The dimensionless parameters of the system are listed as follows:

$$A = H/R, \quad \mathrm{Gr} = g\beta R^3 \Delta T/\nu^2, \quad \mathrm{Pr} = \nu/\alpha, \quad \mathrm{Da} = K/R^2, \quad \mathrm{Fs} = b/R$$

where A, Gr, Pr, Da and Fs denote aspect ratio, Grashof number, Prandtl number, Darcy number and Forchheimer number, respectively. H is the internal height of the autoclave, R is the internal radius of the autoclave, g is the acceleration due to gravity, ΔT is the maximum temperature difference on the sidewall of the autoclave, ν is kinematic viscosity, α is thermal diffusivity, the permeability of porous matrix $K = d_p^2\varepsilon^3/(150(1-\varepsilon)^2)$ with d_p as the average diameter of the nutrient particles, and the Forchheimer coefficient $b = (1.75/(\sqrt{150}\varepsilon^{1.5}))K^{0.5}$.

The governing equations in the porous and fluid layers can be combined by defining a binary parameter B as $B=0$ in the fluid layer and $B=1$ in the porous layer. The porosity $\varepsilon=0$ in solid, $0<\varepsilon<1$ in porous layer and $\varepsilon=1$ in fluid layer. The combined governing equations in a cylindrical coordinate system are

$$\frac{\partial(\varepsilon\rho_f)}{\partial t} + \nabla(\rho_f \mathbf{u}) = 0 \tag{1}$$

$$\frac{\rho_f}{\varepsilon}\frac{\partial \mathbf{u}}{\partial t} + \frac{\rho_f}{\varepsilon}(\mathbf{u}\nabla)\frac{\mathbf{u}}{\varepsilon} = -\nabla p - \rho_f\beta(T-T_0)\mathbf{g} + \nabla(\mu_e\nabla\mathbf{u}) - B\left[\left(\frac{\mu_f}{K} + \frac{\rho_f b}{K}|\mathbf{u}|\right)\mathbf{u}\right] \tag{2}$$

$$(\rho c_p)_e\frac{\partial T}{\partial t} + (\rho c_p)_f[(\mathbf{u}\nabla)T] = \nabla(k_e\nabla T) \tag{3}$$

where μ, k and c_p denote dynamic viscosity, thermal conductivity and specific heat, respectively. $\mathbf{g}$ is the gravity vector. Subscripts f and e denote fluid and effective, respectively.

The following scales are used to non-dimensionalize the governing equations: length, R; velocity, $u_0=\nu/R$; time, $t_0=R^2/\nu$; pressure, $\rho\nu^2/R^2$ and temperature, T_H-T_L. T_H and T_L are the high temperature and low temperature applied on the sidewall of the autoclave, respectively. The resulting non-dimensionalized equations are

$$\frac{\partial\varepsilon\overline{\rho}}{\partial t} + \frac{1}{r}\frac{\partial}{\partial r}(r\overline{\rho}u) + \frac{\partial}{\partial z}(\overline{\rho}w) = 0 \tag{4}$$

$$\frac{\partial}{\partial t}\left(\frac{1}{\varepsilon}\overline{\rho}u\right) + \frac{1}{r}\frac{\partial}{\partial r}\left(\frac{1}{\varepsilon^2}r\overline{\rho}uu\right) + \frac{\partial}{\partial z}\left(\frac{1}{\varepsilon^2}\overline{\rho}wu\right) = \overline{\mu}\left[\frac{1}{r}\frac{\partial}{\partial r}\left(r\frac{\partial u}{\partial r}\right) + \frac{\partial^2 u}{\partial z^2} - \frac{u}{r^2}\right] - \frac{\partial p}{\partial r} - B\left(\frac{1}{\mathrm{ReDa}} + \frac{\mathrm{Fs}}{\mathrm{Da}}|\mathbf{u}|\right)u \tag{5}$$

$$\frac{\partial}{\partial t}\left(\frac{1}{\varepsilon}\overline{\rho}w\right) + \frac{1}{r}\frac{\partial}{\partial r}\left(\frac{1}{\varepsilon^2}r\overline{\rho}uw\right) + \frac{\partial}{\partial z}\left(\frac{1}{\varepsilon^2}\overline{\rho}ww\right) = \overline{\mu}\left[\frac{1}{r}\frac{\partial}{\partial r}\left(r\frac{\partial w}{\partial r}\right) + \frac{\partial^2 w}{\partial z^2}\right] - \frac{\partial p}{\partial z} + \mathrm{Gr}\Theta - B\left(\frac{1}{\mathrm{ReDa}} + \frac{\mathrm{Fs}}{\mathrm{Da}}|\mathbf{u}|\right)w \tag{6}$$

$$\overline{\rho}\overline{c}_p\frac{\partial\Theta}{\partial t} + \frac{1}{r}\frac{\partial}{\partial r}(r\overline{\rho}u\Theta) + \frac{\partial}{\partial z}(\overline{\rho}w\Theta) = \frac{1}{\mathrm{Pr}}\overline{k}\left[\frac{1}{r}\frac{\partial}{\partial r}\left(r\frac{\partial\Theta}{\partial r}\right) + \frac{\partial}{\partial z}\left(\frac{\partial\Theta}{\partial z}\right)\right] \tag{7}$$

where $\overline{\rho} = (\rho_e/\rho_f)$, $\overline{\mu} = (\mu_e/\mu_f)$, $\overline{c}_p = (c_{pe}/c_{pf})$, $\overline{k} = (k_e/k_f)$

The momentum Eqs. (5) and (6) and energy Eq. (7) are solved using an in-house developed finite volume algorithm [14]. A temperature profile is set on the sidewall of the autoclave, $T=T_H$ for $z<H_B-0.5\delta T$; $T=T_H-(T_H-T_L)[z-(H_B-0.5\delta T)]/\delta T$ for $H_B-0.5\delta T\le z\le H_B+0.5\delta T$; $T=T_L$ for $z>H_B+0.5\delta T$, where H_B is the height of the baffle, and δT is the height of the wall where the temperature changes from T_H to T_L. The top and bottom of the autoclave are considered adiabatic. The temperature distribution is considered axisymmetric, $\partial T/\partial r=0$ at $r=0$.

For solving the momentum equations and the pressure equation inside the autoclave, we search the fluid boundaries inside the autoclave in the r and z directions, respectively. For example, when solving the equations using the TDMA method, we search the fluid boundaries in r or z direction separately, and solve the equations in this direction in different intervals of fluid space. This way, we can obtain the fluid field inside the autoclave that contains different shapes of baffles and seeds. For solving the temperature equation, the computational domain includes the autoclave and the charge inside the autoclave. The mesh size of 92×322 in radial and vertical directions is used in the simulation, and the time step is $dt/t_0=10^{-7}$.

3. Results

In order to investigate the effect of different openings of baffle on the flow rate, the autoclaves with six different baffle openings were simulated. Fig. 2 shows the volume flux with different baffle openings of 6%, 8%, 10%, 12%, 16% and 20% where the center hole and the ring gap have equal size. It can be seen that, for opening of 6%, the flow oscillates at high frequency and the volume flux in the center hole is only 2×10^{-6} m^3/s. A flux balance is hard to achieve for a long time. For openings of 8% and 10%, oscillating frequency is less than that of 6%. High frequency oscillation is adverse to crystal growth. Raw materials are easy to deposit on the wall. In the cases

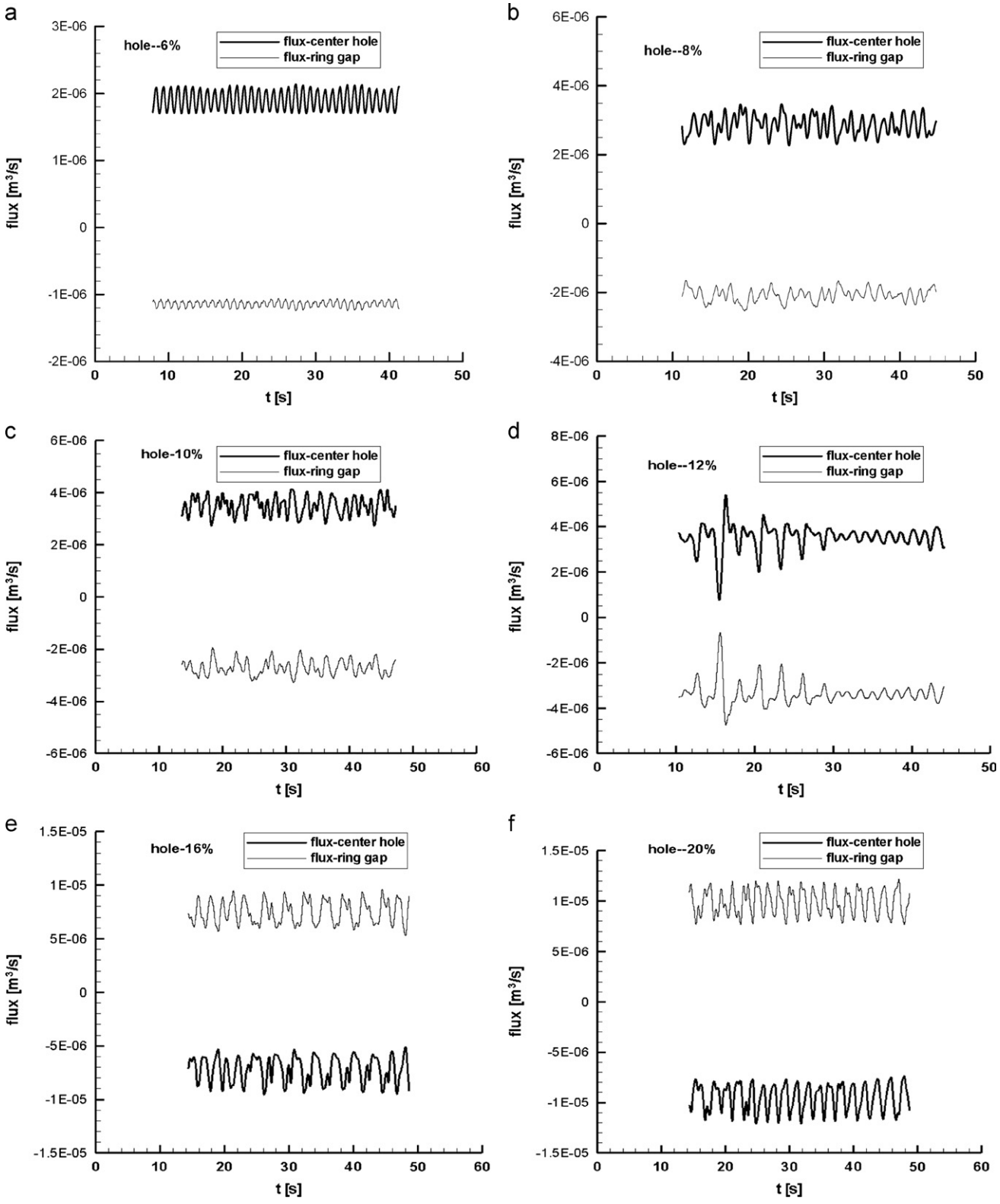

Fig. 2. Volume flux with different baffle openings of (a) 6%, (b) 8%, (c) 10%, (d) 12%, (e) 16% and (f) 20%.

of 6%, 8% and 10% baffle openings, the fluid flow is an oscillatory flow in the whole high-pressure autoclave. The average velocity is positive in the center hole, while in the gap ring it is negative. An oscillatory flow is not good to GaN crystal growth process because raw materials cannot be transported to the vicinity of the seeds. When the opening reaches to 12%, the amplitude of flow oscillation is much larger. In the cases of 16% and 20% openings, the flow direction changes, in which the average flow velocity is negative in the center hole. The fluid flow is a circulating flow, which is in favor of the transfer of raw material.

It can be observed from Fig. 3 that with the increase in the baffle opening from 6% to 8%, volumetric flow rate increases. However,

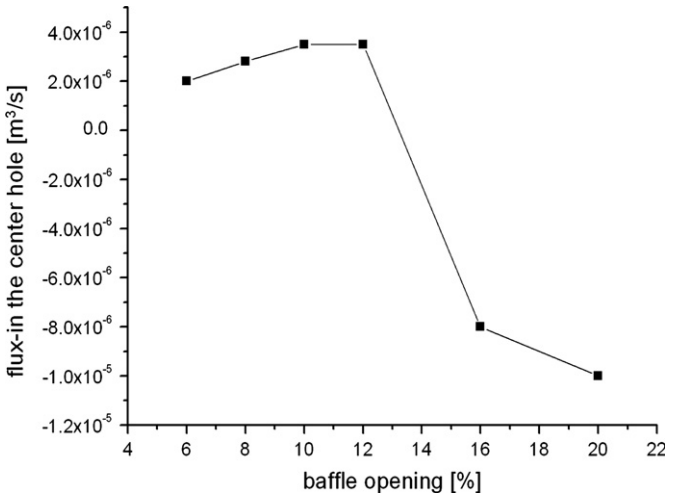

Fig. 3. Volumetric flow rate in the center hole with different baffle openings.

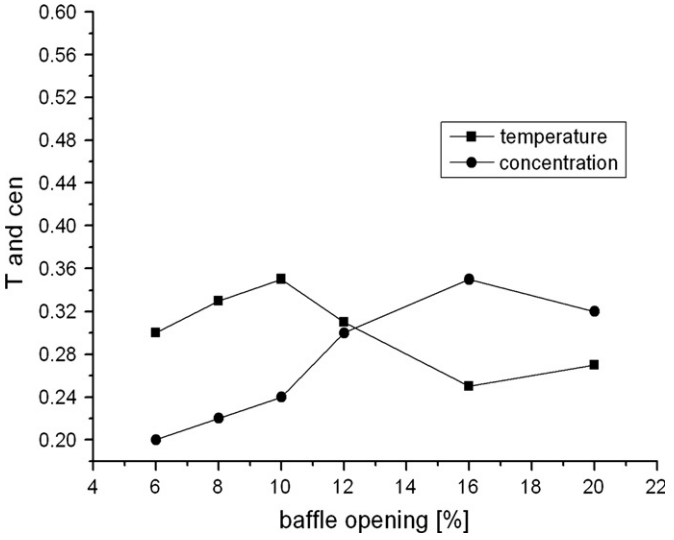

Fig. 4. Temperature and concentration at one point with different baffle openings.

when the opening increases from 10% to 12%, the average volumetric flow rate remains approximately constant. The average volumetric flow rate also increases with the increase of baffle opening from 16% to 20%. The average volumetric flow rate in condition of 20% reaches a maximum.

Fig. 4 shows the relative temperature and concentration at one point close to seed crystal as a function of opening. It can be seen that the relative temperature decreases when the opening varies from 6% to 16%, however, which increases as the opening greater than 16%, because the solute in the dissolving zone and growth zone cannot form circulation as the opening is small. Furthermore, the temperature of fluid in the vicinity of seed crystal increases when the opening increases from 6% to 10%. As the opening is 16%, the flow direction at the central hole is from the low temperature zone to the high-temperature zone, and the low temperature fluid is transported to the seed crystal zone; therefore the temperature of the seed crystal is lower. The flow velocity is much large as the opening increases to 20%, which is in favor of the mixture of fluid. Thus, the seed crystal temperature in the case of 20% opening is larger than that of 16% opening. From Fig. 4 we can also know that the concentration at one monitoring point in the vicinity of seed increases with the increase in opening, because the crystal growth is influenced by two factors: (1) the temperature difference between the crystal growth zone and dissolving zone and (2) the flow rate between the two zones. The seed temperature in the case of 16% opening is lower, even though the flow rate in the case of 20% opening is larger than that of 16%.

4. Conclusions

We modeled ammonothermal growth of GaN crystal of 1 in. size in a cylindrical high-pressure autoclave and discussed the effects of the different baffle designs. We can conclude that, under the condition of forward solubility, the small opening is not in favor of the crystal growth. When the opening increases from 12% to 16%, the flow direction in the central hole changes from positive to negative. In the case of 16% opening, the flow in the autoclave exhibits a steady circulation; hence the growth is stable. The transfer of raw material depends on the baffle opening and the temperature difference between growth zone and dissolving zone.

Acknowledgements

The research was supported by the National Natural Science Foundation of China (no. 50776098).

References

[1] S. Porowski, MRS Internet Journal of Nitride Semiconductor Research 4S1 (1999) G1.3.
[2] H. Yamane, M. Shimada, T. Sekiguchi, F.J. DiSalvo, Morphology and characterization of GaN single crystals grown in a Na flux, Journal of Crystal Growth 186 (1998) 8–12.
[3] F. Kawamura, M. Morishita, K. Omae, M. Yoshimura, Y. Mori, T. Sasaki, Novel liquid phase epitaxy (LPE) growth method for growing large GaN single crystals: introduction of the flux film coated-liquid phase epitaxy (FFC-LPE) method, Japanese Journal of Applied Physics 42 (2003) L879–L881.
[4] R. Dwilinski, J.M. Baranowski, M. Kaminska, R. Doradzinski, J. Garczynski, L. Sierzputowski, On GaN crystallization by ammonothermal method, Acta Physics Polonica A 90 (4)(1996) 763–766.
[5] R. Dwilinski, R. Doradzinski, J. Garczynski, L. Sierzputowski, M. Palczewska, A. Wysmolek, M. Kaminska, MRS Internet Journal of Nitride Semiconductor Research 3 (1998) 25–31.
[6] D.R. Ketchum, J.W. Kolis, Crystal growth of gallium nitride in supercritical ammonia, Journal of Crystal Growth 222 (3)(2001) 431–434.
[7] A.P. Purdy, Ammonothermal synthesis of cubic gallium nitride, Chemistry of Materials 11 (7)(1999) 1648–1651.
[8] A. Yoshikawa, E. Ohshima, T. Fukuda, H. Tsuji, K. Oshima, Crystal growth of GaN by ammonothermal method, Journal of Crystal Growth 260 (1–2)(2004) 67–72.
[9] Q.S. Chen, S. Pendurti, V. Prasad, Effects of baffle design on fluid flow and heat transfer in ammonothermal growth of nitrides, Journal of Crystal Growth 266 (2004) 271–277.
[10] Q.S. Chen, S. Pendurti, V. Prasad, Modeling of ammonothermal growth of gallium nitride single crystals, Journal of Materials Science 41 (2006) 1409–1414.
[11] Q.S. Chen, V. Prasad, W.R. Hu, Modeling of ammonothermal growth of nitrides, Journal of Crystal Growth 258 (2003) 181–187.
[12] S. Pendurtia, Q.S. Chen, V. Prasad, Modeling ammonothermal growth of GaN single crystals: The role of transport, Journal of Crystal Growth 296 (2006) 150–158.
[13] Y. Masuda, A. Suzuki, Y. Mikawa, Y. Kagamitani, T. Ishiguro, C. Yokoyama, T. Tsukada, Numerical simulation of GaN single-crystal growth process in ammonothermal autoclave—effects of baffle shape, International Journal of Heat and Mass Transfer 53 (2010) 940–943.
[14] Q.S. Chen, V. Prasad, A. Chatterjee, Modeling of fluid flow and heat transfer in a hydrothermal crystal growth system: use of fluid-superposed porous layer theory, ASME Journal of Heat Transfer 21 (1999) 1049–1058.